Extreme hyperopia is the result of null mutations in *MFRP*, which encodes a Frizzled-related protein

Olof H. Sundin[a,b,c], Gregory S. Leppert[a,d], Eduardo D. Silva[a,e,f], Jun-Ming Yang[a,g], Sharola Dharmaraj[a,e,h], Irene H. Maumenee[e], Luisa Coutinho Santos[i], Cameron F. Parsa[j], Elias I. Traboulsi[k], Karl W. Broman[l], Cathy DiBernardo[m], Janet S. Sunness[m,n], Jeffrey Toy[a,o], and Ethan M. Weinberg[a]

[a]Laboratory of Developmental Genetics, [e]Johns Hopkins Clinic for Hereditary Eye Diseases, [j]Krieger Center for Pediatric Ophthalmology, [m]Ocular Imaging and Low Vision Clinics, Wilmer Eye Institute, [b]Department of Molecular Biology and Genetics, School of Medicine, and [l]Department of Biostatistics, Bloomberg School of Public Health, The Johns Hopkins University, Baltimore, MD 21287; [f]Department of Ophthalmology, University of Coimbra, 3000-033 Coimbra, Portugal; [i]Instituto de Oftalmologia Dr. Gama Pinto, 1169-019 Lisbon, Portugal; and [k]Cole Eye Institute, Cleveland Clinic Foundation, Cleveland, OH 44195

Nanophthalmos is a rare disorder of eye development characterized by extreme hyperopia (farsightedness), with refractive error in the range of +8.00 to +25.00 diopters. Because the cornea and lens are normal in size and shape, hyperopia occurs because insufficient growth along the visual axis places these lensing components too close to the retina. Nanophthalmic eyes show considerable thickening of both the choroidal vascular bed and scleral coat, which provide nutritive and structural support for the retina. Thickening of these tissues is a general feature of axial hyperopia, whereas the opposite occurs in myopia. We have mapped recessive nanophthalmos to a unique locus at 11q23.3 and identified four independent mutations in *MFRP*, a gene that is selectively expressed in the eye and encodes a protein with homology to Tolloid proteases and the Wnt-binding domain of the Frizzled transmembrane receptors. This gene is not critical for retinal function, as patients entirely lacking *MFRP* can still have good refraction-corrected vision, produce clinically normal electroretinograms, and show only modest anomalies in the dark adaptation of photoreceptors. *MFRP* appears primarily devoted to regulating axial length of the eye. It remains to be determined whether natural variation in its activity plays a role in common refractive errors.

eye | genetics | morphology | nanophthalmos

Fig. 1. Morphological features of nanophthalmos. A diagram of the eye, sagittal section, and light path is shown. (*A*) Normal, closer view. (*B*) Nanophthalmic. Adapted from ref. 4 to reflect eye morphology of individual 7 in kindred A.

The general problem of how organs in the body regulate their size is illustrated by the human eye, which during postnatal growth normally maintains the distance between cornea and fovea to within 2% of its optimal focal length (1). Studies in birds and mammals have revealed that this process is driven by visual experience. Focus quality is evaluated locally within the retina, which in turn signals underlying tissues to promote or restrict elongation of the optic axis (2). The use of mouse genetics to identify essential components of the underlying mechanism has, so far, not been feasible because this species appears unable to adjust ocular focus by regulating axial growth (3).

To approach this problem, we have mapped and identified a mutation causing nanophthalmos, a rare human genetic disorder in which both eyes are small, functional, and without major structural faults (1, 4, 5). The cornea and lens are normal in size and refractive power, but the distance from lens to retina is unusually short. This places the focal point of the eye well behind the retina (Fig. 1*B*), causing a hyperopic refractive error of +8.00 diopters or more. Additional characteristics are a narrow angle between the iris and cornea, expansion of the choroidal vascular bed underlying the retinal pigment epithelium (RPE), and thickening of the scleral connective tissue surrounding the eye. More moderate examples of these same histological changes are found in high hyperopia (1, 6), which differs from nanophthalmos only in degree.
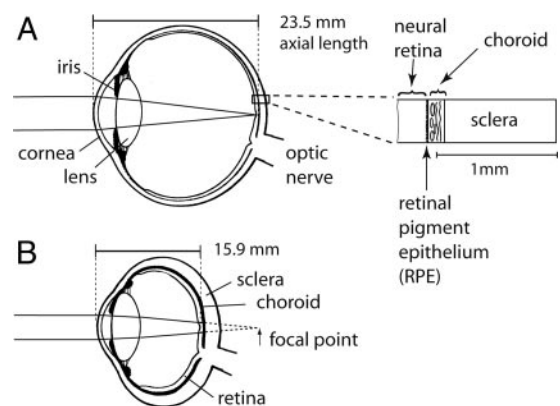
Secondary complications are common with extreme hyperopia, in which supporting tissues of the developing eye reach less than half their normal area, yet must accommodate growth of a full-sized neural retina. This lateral crowding causes localized slippage between retina and RPE, leading to deformation or loss of the foveal pit and the formation of crescent-shaped macular folds, both of which impair visual acuity (7, 8). As adults, additional complications can develop, including angle closure glaucoma, cystic edema, and retinal detachment. The thick scleral connective tissue is thought to constrict outflow vessels of the choroidal vascular bed, causing accumulation of fluid between RPE and retina, which in turn drives retinal detachment. Glaucoma occurs when the forwardly displaced iris obstructs passages in the corneal margin, which
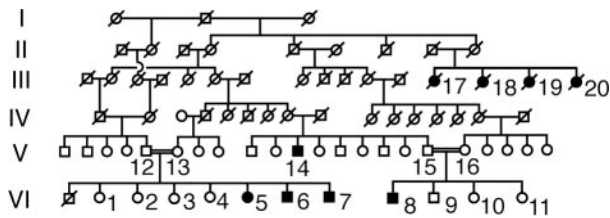
Fig. 2. Inheritance of nanophthalmos. Kindred A, showing individuals relevant to the current study, and participants in an earlier study (patients 17–19) (10) are shown. All offspring are shown only in VI.

are needed for the outflow of aqueous humor, leading to elevated pressure within the eye (4).

Nanophthalmos is typically sporadic and rare. A dominantly inherited form maps to the *NNO1* locus (Online Mendelian Inheritance in Man accession no. 600165), a 27-megabase (Mb) interval of chromosome 11 (9). Although the *NNO1* gene remains unknown, one candidate is *VMD2*, the Best's macular dystrophy gene, in which a small subset of splicing mutations cause syndromic vitreoretinopathy accompanied by nanophthalmos (10). Large families showing recessive or semidominant inheritance of nonsyndromic nanophthalmos are known (5, 6, 11–13), but no loci have been reported. This article describes a locus for recessive nanophthalmos and its association with mutations in the *MFRP* gene.

Materials and Methods

Human Subjects and Clinical Examinations. Informed consent was obtained and research was conducted in accord with the Declaration of Helsinki at The Johns Hopkins University, University of Coimbra, Instituto Gama Pinto, and the Cole Eye Institute. Standard clinical exams evaluated visual acuity, objective refraction with cycloplegia, immersion A-scan ultrasonography, and electroretinography (ERG). Dark adaptation used a Goldmann-Weekers dark adaptometer or an equivalent visual stimulus set up in an LKC Technologies (Gaithersburg, MD) Ganzfeld apparatus.

Genotypes and Genetic Linkage Analysis. Human genomic DNA was obtained from buccal epithelium or blood as described (14). For manual genotyping of 366 autosomal tandem repeat polymorphisms, we used ^{32}P end-labeled CHLC/Weber version 9 primers (Research Genetics, Huntsville, AL) (15). More markers were obtained from the Marshfield genetic maps (16). For each marker, amplimers of subjects 1–16 (Fig. 2), two CEPH-Généthon DNA standards, and a sequence ladder were run on the same gel. Two-point linkage was obtained with LIPED (17), assuming recessive inheritance and full penetrance. Marker allele frequencies were taken from CEPH genotype data, where available, or estimated from current data (18).

Exon and Genomic Sequencing to Detect Mutations. Amplification of exons from genomic DNA was as described (14), followed by automated sequencing with dye terminators. Primer sequences and a map are available in *Supporting Text* and Fig. 7, which are published as supporting information on the PNAS web site. Amplimers of normal controls were tested for Q175X by BstN1 digestion and for 1143insC, 492delC, or I182T by T-track sequencing.

Results

Recessive Inheritance of Extreme Axial Hyperopia. A 30-year-old woman presented with nanophthalmos, angle closure glaucoma, and massive retinal detachment in the left eye (Figs. 2 and 3*D*, patient 5). Four other members of her Amish-Mennonite kin-

dred were also affected by nanophthalmos, but had neither glaucoma nor retinal detachment. Inheritance followed an autosomal recessive pattern. In addition, three deceased relatives (Fig. 2, patients 17–19) had been described in a classic study of nanophthalmos by Cross and Yoder (11). Outwardly, affected eyes showed prominent forward bowing of the iris and a narrow angle between iris and cornea (Fig. 3*A*). Diameter and curvature of the cornea were within normal range.

Examination of the retina revealed absence of a normal foveal pit, presence of macular folds (7, 8), and slight tortuosity of blood vessels in patients 7 (Fig. 3 *B* and *C*) and 8 and the left eye of patient 6. Aside from these common secondary effects of extreme hyperopia, these retinas appeared healthy, with the exception of patches of hypopigmentation in the lateral fundus (Fig. 3*C*, arrows). There was no evidence of the distinctive RPE pigment clumping that accompanies photoreceptor degeneration (5). This eye had a refractive error of +14.50, an unusually short axial length of 15.45 mm, and visual acuity of 20/40 with glasses (Fig. 3*D*). Ultrasonography (Fig. 3*E*) revealed forward placement of a slightly longer lens, a vitreous cavity of half normal length, and 3.3 times the normal thickness of sclera and choroid (1, 4). Those affected had extreme hyperopia and short axial lengths, whereas parents and unaffected siblings showed normal variation, suggesting a fully recessive mutation.

Lens-corrected visual acuity of these patients ranged from normal (20/20) to very poor (20/200) and appeared correlated with secondary consequences of extreme hyperopia, such as foveal deformation, retinal folds, and macular edema. The right eye of patient 6 had a normally shaped foveal pit, as indicated by a distinctive optical reflection. This may explain 20/20 visual acuity of this eye and opens the possibility that the acuity deficits seen in others were caused entirely by secondary conditions affecting retinal structure, rather than by a primary dysfunction of photoreception. The most mildly affected, an uncle, age 65, had hyperopia of +9.75, strabismus, early cataracts, normal foveal pits, and no signs of retinal hypopigmentation (Fig. 3*D*, patient 14).

ERG and Dark Adaptation. ERG tests, which measure light-evoked primary electrical responses of photoreceptors (A-waves) and secondary responses of other retinal cells (B-waves), were clinically normal for patients 5 and 7. Amplitudes of the rod photoreceptor response to dim light were near the low end of the normal range, whereas cone photoreceptor responses were stronger. Response times of both rods and cones and of other cells were completely normal (Fig. 3*F*). Dark-adaptation kinetics revealed moderate anomalies. For patient 7, cone photoreceptors adapted significantly more slowly, and once dark-adapted, they were 10 times less sensitive than normal (Fig. 3*G*). Rods also adapted more slowly, although once dark-adapted they were as sensitive to dim light as a normal eye. Patient 5 showed a similar delay in the adaptation of rod photoreceptors, which were five times less sensitive once adapted. Surprisingly, her cone adaptation appeared identical to the control, both in rate or dark-adapted threshold.

Genetic Linkage to 11q23.3. To map the disease, we genotyped DNA samples from family members 1–16 (Fig. 2) by using short tandem repeat markers. A logarithm of odds score of 5.95 at *D11S1341* and >3.0 at three nearby loci established linkage to 11q23.3 (Fig. 4*A*). All nanophthalmos patients in generation VI shared a single homozygous haplotype between *D11S939* and *D11S912* (Fig. 5). A crossover in the maternal chromosome of one unaffected sister (patient 2) placed the disease locus above *D11S4132*, defining a 2.14-Mb disease interval between *D11S939* and *D11S4132*. The uncle, patient 14, was heterozygous for this interval, but homozygous within a 383-kb subregion (Fig. 4*B*).
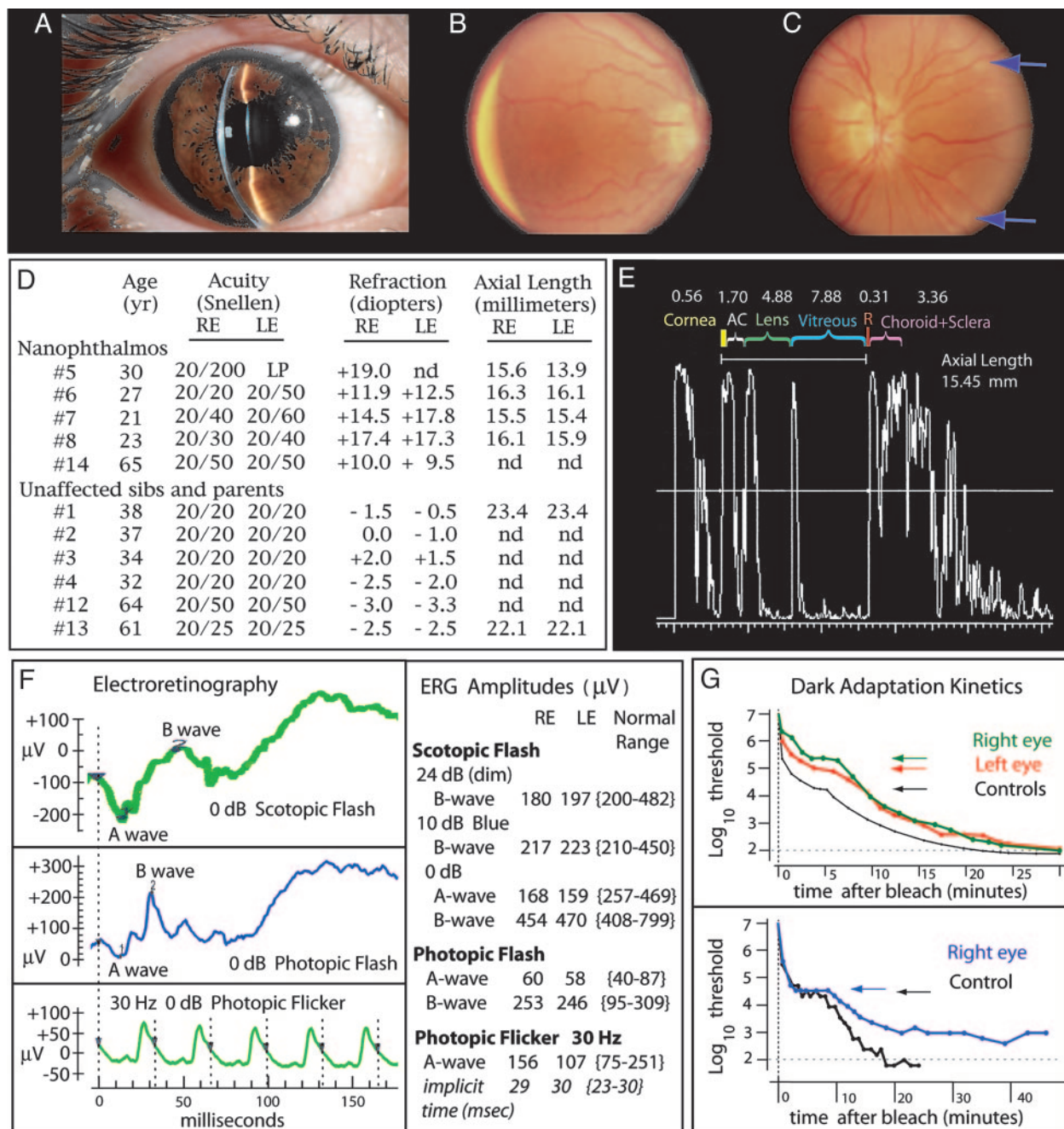
Fig. 3. Clinical features of nanophthalmos in kindred A. (*A*) Right eye (RE) of patient 5, with vertical slit lamp illumination. (*B*) Central retinal fundus, RE of patient 7. (*C*) Lateral retina, RE of patient 7. (*D*) Ocular features of individuals 1–16. Refraction indicates spherical +1/2 cylindrical. LE, left eye; nd, not determined. (*E*) A-scan immersion ultrasound, RE of patient 7. Shown are the return times of echo peaks along the optic axis. An interpretation, in mm, is based on 10 independent scans. (*F Left*) ERG tracings, RE of patient 7. Time of a brief whole-field flash administered in the dark to a dark-adapted eye (scotopic) is indicated by vertical dashed lines. Electrical response of the retina, as measured between body and cornea, is indicated in μV. A bright flash over background illumination (photopic) or a repeating train of flashes was used to isolate cone responses. (*F Right*) Results from a second clinical examination of patient 7, indicating peak amplitudes in μV for A-waves (photoreceptor hyperpolarization) and B-waves (postsynaptic depolarization of retina). (*G*) (*Upper*) Dark-adaptation kinetics. Visual pigment of the whole eye is bleached by 5 min of bright white light (1,000 candelas per m^2). Time in darkness immediately after the bleaching is indicated on the *x* axis. The *y* axis indicates minimum light intensity in microapostilbs that can be seen by the subject at a given time. The testing stimulus for rods and cones is a flashing disk 7° in diameter, placed 15° below a dim red focal target. (*Lower*) Dark adaptation, RE of patient 5, using LKC Technologies Ganzfeld.

Independent Null Mutations in a Membrane-Type Frizzled-Related Protein (MFRP). Exons of 13 genes in the 383-kb interval (Fig. 4*B*) revealed homozygous polymorphic variants, but no mutations. Returning to the larger interval, we screened *MFRP*, a 13-exon gene encoding MFRP (19). Exon 10 of *MFRP* contained a frameshift insertion, 1143insC, that was homozygous in all of those affected in

generation VI (Fig. 6*A*). This mutation truncated the protein at glycine 383 and added seven frameshift codons. It was not found in 750 normal controls. Patient 14 was heterozygous for the 1143insC allele but had no other mutations in exons of *MFRP* or *C1QTNF5*, an adjoining retinopathy gene (20).

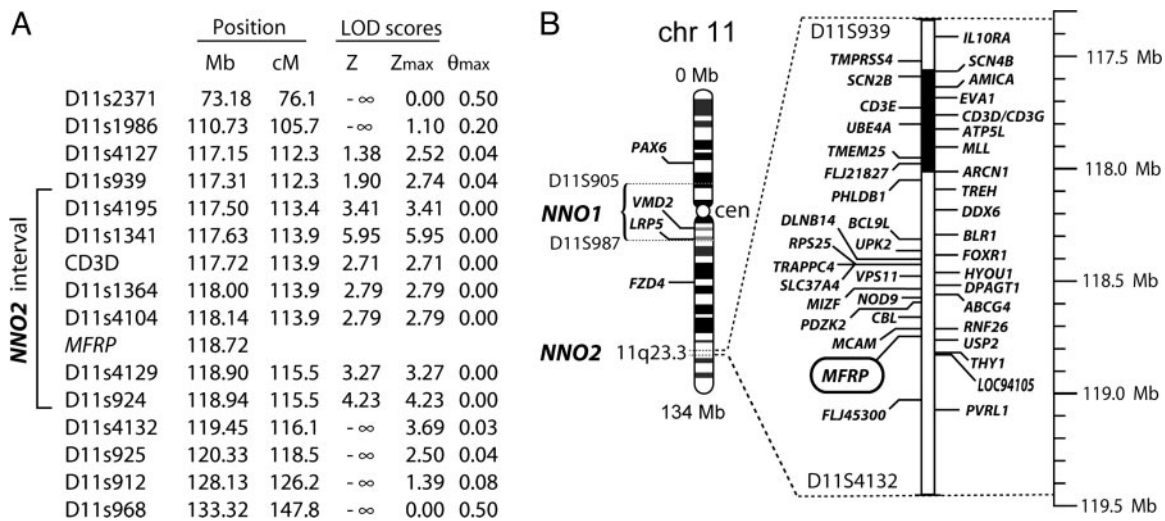After screening 26 independent nanophthalmos kindreds, two

Fig. 4. Genetic linkage to the *NNO2* disease locus. (*A*) Chromosomal position marked in Mb and cM. Two-point logarithm of odds (LOD) scores are shown. For Z, at $\theta = 0$ (mutation coincident with marker), and for Z_{max}, maximum LOD score, at θ_{max} (recombination frequency between mutation and marker). (*B*) Map of 2.14-Mb disease interval and known genes, homozygous for all affected in generation VI. Black bar indicates 383-kb interval homozygous in patient 14.

Caucasian families revealed mutations in *MFRP*. A boy, age 9, was homozygous for Q175X, an amber mutation in exon 5, whereas each parent was heterozygous for the mutation (Fig. 6*B*). His refractive error was +13.40 and +13.60, with 20/80 acuity in each eye. The RPE showed no pigmentary anomalies. In the second family, two sisters, ages 28 and 25, had average refractive errors of +22.00 and +22.25. Each had patches of RPE hypopigmentation in the lateral retina. Both sisters were compound heterozygotes for 492delC, a frameshift deletion, and I182T in exon 5 (Fig. 6*C*). Q175X, 492delC, and I182T were not found in 118 normal Caucasians.

Three mutations truncated MFRP in one of the cubilin domains and removed the cysteine-rich domain (CRD) (Fig. 6*D*). I182T substituted threonine at an extremely conserved hydrophobic site, one of which is retained as isoleucine in cubilin

domains of very different proteins, including CUBN, TLL1, LRP3, and the serum complement subunit C1S. An alignment illustrating this is shown in *Supporting Text*. Buried within the C1S structure (see *Supporting Text* and Fig. 8, which is published as supporting information on the PNAS web site), this isoleucine makes contact with conserved hydrophobic residues of two closely apposed β-sheets (Protein Data Bank ID code 1NZI). Substitution of a polar threonine would likely destabilize the structure.

Discussion

MFRP. MFRP (19) has no close relative elsewhere in the genome. However, portions show homology to individual domains of genes involved in cell–cell signaling, endocytosis, and proteolysis. Its C-terminal domain is related to the Wnt-binding CRD
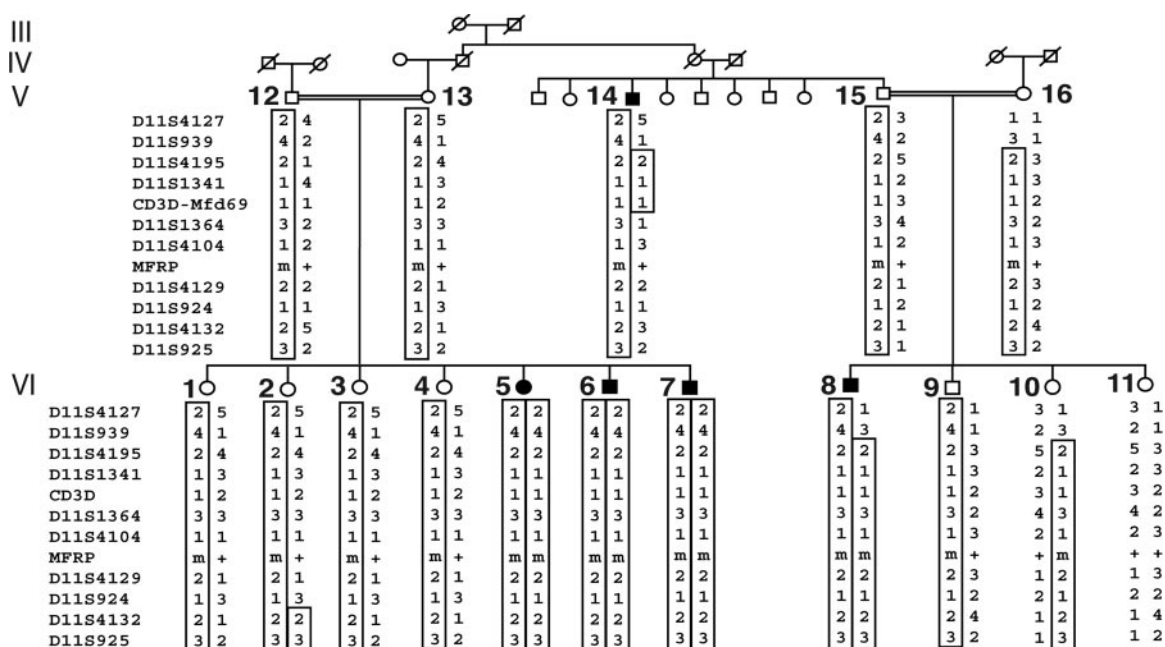

Fig. 5. Haplotypes. Chromosome 11 marker allele haplotypes for the linkage pedigree are shown below genotyped individuals. Boxes contain haplotypes of the disease chromosome.
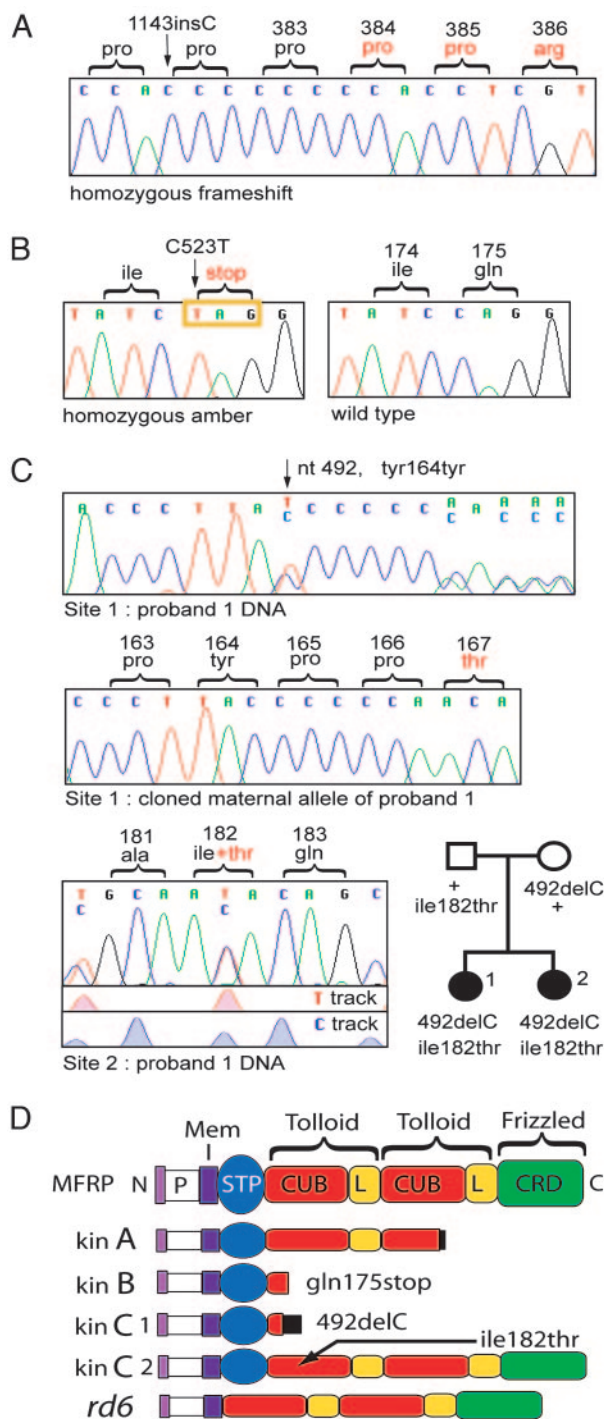
Sundin *et al.*

Fig. 6. Mutations in *MFRP*. (*A*) Automated sequencing trace of a homozygous exon 10 mutation in the Amish-Mennonite kindred. (*B*) A homozygous exon 5 amber stop codon mutation in the proband from kindred B. (*C*) Compound heterozygosity in exon 5 shows a frameshift deletion and a point substitution in two affected sisters of kindred C. (*D*) Diagram of normal MFRP (top row). Below are encoded mutant proteins in kindreds A–C and mouse *rd6*. N, amino terminus; C, carboxyl terminus; P, proline-rich interval; Mem, membrane spanning helix; STP, serine-threonine-proline-rich interval; CUB, cubilin-related; L, low-density lipoprotein receptor-related. CRD, Frizzled-related CRD.

of the Frizzled family of transmembrane proteins (21). Frizzled proteins are receptors for the Wnts, a family of cell–cell signaling molecules that mediate the regulation of growth, differentiation,

and cell polarity during development (22). Mutations in *FZD4* and some alleles of *LRP5*, which encodes its coreceptor, cause the vascular eye disease familial exudative vitreo-retinopathy (23). Mutations in *LRP5* typically cause pseudoglioma and vascular defects in the fetal eye and affect bone accrual (24). The Norrie disease gene encodes a non-Wnt ligand of FZD4, one that is essential to eye and ear development (25). Secreted Frizzled-related proteins, which contain homologues of the Wnt-binding CRD (26), are thought to act as competitive inhibitors of Wnt signaling, and a similar function has been proposed for MFRP (19, 27). However, this idea is still speculative, because MFRP binding to Wnt proteins has yet to be demonstrated. Other roles are suggested by its closest CRD homologue, corin, a membrane-bound protease that cleaves the precursor of atrial natriuretic factor (28). Although MFRP has no obvious peptidase catalytic site, involvement in proteolytic pathways is also suggested by two Tolloid repeat units, each of which is comprised of globular domains related to cubulin and the low-density lipoprotein receptor (Fig. 6*D*). These are homologous to the Tolloid metalloproteinase family, which includes BMP1, a regulator of procollagen processing and bone development (29).

Sites of Expression and Function. RNA blot hybridization (19, 27) and public cDNA databases show that *MFRP* and its mouse orthologue are expressed prominently only in the eye and at very low levels in the brain. This result is consistent with our finding that null homozygotes manifested no disease outside of the eye. In the mouse, *in situ* hybridization has revealed substantial *Mfrp* mRNA in the RPE and ciliary body but no other ocular tissues (27). Our preliminary RT-PCR analysis of human and mouse tissues (data not shown) confirms these results, including the absence of expression in choroid and sclera.

On the basis of changes in collagen fibril ultrastructure and sulfated proteoglycan metabolism documented in scleral explants, nanophthalmos has been considered a primary defect of connective tissue (30). Our finding that the disease is caused by loss of a gene expressed in the RPE introduces a different perspective on this disorder. Although the RPE is a very thin tissue layer of the eye (Fig. 1), it plays an important role in regulating differentiation and growth of more massive underlying tissues. In early development, the RPE induces formation of periocular choroid and sclera from undifferentiated neural crest mesenchyme (31). In postnatal development, the retina adjusts ocular focus by altering extensibility of the sclera, and the RPE has been postulated, but not proven, to relay these regulatory signals from the retina (2). Retinoic acid in the retina is markedly decreased during lens-induced hyperopia in mammals (32), and a similar decrease might also occur in nanophthalmos. Because retinoic acid and 11-cis retinal both arise from vitamin A and undergo metabolism in the RPE, the mechanism used to down-regulate retinoic acid synthesis could have secondary effects on the recycling of visual pigment. The moderate and differing delays in dark adaptation observed in the two patients examined (Fig. 3*G*) could reflect secondary deficiencies in the regeneration of 11-cis retinal (33) or availability of vitamin A (34).

Differences in Phenotype Between Human and Mouse. The recessive mouse retinal degeneration mutation *rd6* is a splicing defect in the orthologous *Mfrp* gene that causes an in-frame deletion of exon 4 from the mRNA (27). By 8 weeks of age, *rd6* mice show a myriad of small, round, pigment-free flecks in fundoscopic views of the RPE. These flecks are accompanied by progressive dysfunction and death of photoreceptors. Shed rod outer segments accumulate in the subretinal space, suggesting a possible decrease in phagocytosis by the RPE. The cause of focal depigmentation remains unknown, but appears related to the presence of single large macrophages at the center of each spot. Human *MFRP* disease has larger, irregular patches that retain

partial pigmentation. A more basic difference is the apparent absence of photoreceptor degeneration in our patients or in patients 17, 18, and 19, who, at ages 70, 76 and 78, respectively, had glaucoma and extensive hypopigmentation and no report of night blindness (11).

Although the phenotype of *Mfrp^rd6* mice has been comprehensively described (27, 35, 36), microphthalmia is not part of this description, and sections of *rd6* eyes show a choroid of apparently normal histology and thickness (36). If these mice do have small eyes, the defect is subtle. Because the mouse eye already has an extremely short distance from lens to retina and appears to lack the ability to adjust ocular focus (3), developmental differences between mice and primates may be great enough that mouse *Mfrp* plays no significant role in ocular growth.

Basis of the Affected Heterozygote. As yet, we cannot explain the phenotype of patient 14, the only affected 1143insC heterozygote in kindred A. One possibility is that his nanophthalmos results from digenic interaction of the *MFRP* heterozygote and functional polymorphisms in another gene. Other possibilities are that the trait is semidominant with partial penetrance related to gene dosage and to unknown genetic or environmental factors (37). Alternatively, a rare somatic crossover or uniparental disomy of chromosome 11 in the early embryo could have rendered 1143insC homozygous in the RPE, while leaving the locus heterozygous in buccal epithelium and blood.

The simplest explanation is that patient 14 is a compound heterozygote of 1143insC and a second mutant allele of *MFRP*. A normal fovea, no hypopigmentation, and an average refraction of +9.75 at age 65 suggest that this second mutant allele retains some *MFRP* function. A noncoding mutation, for example, could decrease transcription, splicing, or message stability (37). Because the family was ascertained entirely on the basis of homozygosity for the rare mutation 1143insC, and the second allele is therefore gratuitous, hypomorphic mutations of this type should be more frequent than 2%. Individuals homozygous for this particular hypomorphic allele could be relatively common and should have twice the *MFRP* function of patient 14. They should therefore exhibit more moderate hyperopia, perhaps within the range of common refractive error (1).

1. Duke-Elder, S. (1970) in *Opthalmic Optics and Refraction*, ed. Duke-Elder, S. (Mosby, St. Louis), Vol. 5, pp. 207–300.
2. Wallman, J. & Winawer, J. (2004) *Neuron* **43**, 447–468.
3. Schmucker, C. & Schaeffel, F. (2004) *Vision Res.* **44**, 2445–2456.
4. Singh, O. S. & Sofinski, S. J. (1994) in *Principles and Practice of Ophthalmology*, eds. Albert, D. M. & Jakobiec, F. A. (Saunders, Philadelphia), Vol. 3, pp. 1528–1540.
5. Traboulsi, E. I. (1998) in *Genetic Diseases of the Eye: A Textbook and Atlas*, ed. Traboulsi, E. I. (Oxford Univ. Press, New York), pp. 51–80.
6. Fledelius, H. C., Fuchs, H. J. & Rosenberg, T. (2004) *Optom. Vis. Sci.* **81**, 762–768.
7. Warburg, M. (1979) *Trans. Ophthalmol. Soc. UK* **99**, 272–283.
8. Serrano, J. C., Hodgkins, P. R., Taylor, D. S., Gole, G. A. & Kriss, A. (1998) *Br. J. Ophthalmol.* **82**, 276–279.
9. Othman, M. I., Sullivan, S. A., Skuta, G. L., Crockrell, D. A., Stringham, H. M., Downs, C. A., Fornes, A., Mick, A., Boehnke, M., Vollrath, D. & Richards, J. E. (1998) *Am. J. Hum. Genet.* **63**, 1411–1418.
10. Yardley, J., Leroy, B. P., Hart-Holden, N., Lafaut, B. A., Loeys, B., Messiaen, L. M., Perveen, R., Reddy, M. A., Bhattacharya, S. S., Traboulsi, E., *et al.* (2004) *Invest. Ophthalmol. Visual Sci.* **45**, 3683–3689.
11. Cross, H. E. & Yoder, F. (1976) *Am. J. Ophthalmol.* **81**, 300–306.
12. Altintas, A. K., Acar, M. A., Yalvac, I. S., Kocak, I., Nurozler, A. & Duman, S. (1997) *Acta Ophthalmol. Scand.* **75**, 325–328.
13. MacKay, C. J., Shek, M. S., Carr, R. E., Yanuzzi, L. A. & Gouras, P. (1987) *Arch. Ophthalmol.* **105**, 366–371.
14. Sundin, O. H., Yang, J. M., Li, Y., Zhu, D., Hurd, J. N., Mitchell, T. N., Silva, E. D. & Maumenee, I. H. (2000) *Nat. Genet.* **25**, 289–293.
15. Sheffield, V. C., Weber, J. L., Buetow, K. H, Murray, J. C., Even, D. A., Wiles, K., Gastier, J. M., Pulido, J. C., Yandava, C., Sunden, S. L., *et al.* (1995) *Hum. Mol. Genet.* **4**, 1837–1844.
16. Broman, K. W., Murray, J. C., Sheffield, V. C., White, R. L. & Weber, J. L. (1998) *Am. J. Hum. Genet.* **63**, 861–869.
17. Ott, J. (1974) *Am. J. Hum. Genet.* **26**, 588–597.
18. Broman, K. W. (2001) *Genet. Epidemiol.* **20**, 307–315.
19. Katoh, M. (2001) *Biochem. Biophys. Res. Commun.* **282**, 116–123.
20. Hayward, C., Shu, X., Cideciyan, A. V., Lennon, A., Barran, P., Zareparsi, S., Sawyer, L., Hendry, G., Dhillon, B., Milam, A. H., *et al.* (2003) *Hum. Mol. Genet.* **12**, 2657–2667.
21. Wang, Y., Macke, J. P., Abella, B. S., Andreasson, K., Worley, P., Gilbert, D. J., Copeland, N. G., Jenkins, N. A. & Nathans, J. (1996) *J. Biol. Chem.* **271**, 4468–4476.
22. Bhanot, P., Brink, M., Samos, C. H., Hsieh, J. C., Wang, Y., Macke, J. P., Andrew, D., Nathans, J. & Nusse, R. (1996) *Nature* **382**, 225–230.
23. Robitaille, J., MacDonald, M. L., Kaykas, A., Sheldahl, L. C., Zeisler, J., Dube, M. P., Zhang, L. H., Singaraja, R. R., Guernsey, D. L., Zheng, B., *et al.* (2002) *Nat. Genet.* **32**, 326–330.
24. Gong, Y., Slee, R. B., Fukai, N., Rawadi, G., Roman-Roman, S., Reginato, A. M., Wang, H., Cundy, T. J., Glorieux, F. H., Lev, D., *et al.* (2001) *Cell* **107**, 513–523.
25. Xu, Q., Wang, Y., Dabdoub, A., Smallwood, P. M., Williams, J., Woods, C., Kelley, M. W., Jiang, L., Tasman, W., Zhang, K. & Nathans, J. (2004) *Cell* **116**, 883–895.
26. Kawano, Y. & Kypta, R. (2003) *J. Cell Sci.* **116**, 2627–2634.
27. Kameya, S., Hawes, N. L., Chang, B., Heckenlively, J. R., Naggert, J. K. & Nishina, P. (2002) *Hum. Mol. Genet.* **11**, 1879–1886.
28. Knappe, S., Wu, F., Madlansacay, M. R. & Wu, Q. (2004) *J. Biol. Chem.* **279**, 34464–34471.
29. Sarras, M. P. (1996) *BioEssays.* **18**, 439–442.
30. Yue, B. Y., Duvall, J., Goldberg, M. F., Puck, A., Tso, M. O. M. & Sugar, J. (1986) *Ophthalmology* **93**, 534–541.
31. Seko, Y., Tanaka, Y. & Tokoro, T. (1994) *Graefes Arch. Clin. Exp. Ophthalmol.* **232**, 545–552.
32. McFadden, S. A., Howlett, M. H. C. & Mertz, J. R. (2004) *Vision Res.* **44**, 643–653.
33. Yamamoto, H., Simon, A., Eriksson, U., Harris, E., Berson, E. L. & Dryja, T. P. (1999) *Nat. Genet.* **22**, 188–191.
34. Lamb, T. D. & Pugh, E. N. (2004) *Progr. Ret. Eye Res.* **23**, 307–380.
35. Hawes, N. L., Chang, B., Hageman, G. S., Nusinowitz, S., Nishina, P. M., Schneider, B. S., Smith, R. S., Roderick, T. H., Davisson, M. T. & Heckenlively, J. R. (2000) *Invest. Ophthalmol. Visual Sci.* **41**, 3149–3157.
36. Chang, B., Hawes, N. L., Hurd, R. E., Davisson, M. T., Nusinowitz, S. & Heckenlively, J. R. (2002) *Vision Res.* **42**, 517–525.
37. Nadeau, J. H. (2001) *Nat. Rev. Genet.* **2**, 165–174.